PHYSICAL REVIEW E

STATISTICAL PHYSICS, PLASMAS, FLUIDS, AND RELATED INTERDISCIPLINARY TOPICS

THIRD SERIES, VOLUME 58, NUMBER 6 PART A DECEMBER 1998

RAPID COMMUNICATIONS

The Rapid Communications section is intended for the accelerated publication of important new results. Since manuscripts submitted to this section are given priority treatment both in the editorial office and in production, authors should explain in their submittal letter why the work justifies this special handling. A Rapid Communication should be no longer than 4 printed pages and must be accompanied by an abstract. Page proofs are sent to authors.

Tests of conformal invariance in randomness-induced second-order phase transitions

Christophe Chatelain and Bertrand Berche*

Laboratoire de Physique des Matériaux, Université Henri Poincaré, Nancy 1, Boîte Postale 239, F-54506 Vandœuvre les Nancy Cedex, France

(Received 6 July 1998; revised manuscript received 29 September 1998)

The conformal covariance of correlation functions is checked in the second-order transition induced by random bonds in the two-dimensional eight-state Potts model. The decay of correlations is obtained *via* transfer matrix calculations in a cylinder geometry, and large-scale Monte Carlo simulations provide access to the correlations and the profiles inside a square with free or fixed boundary conditions. In both geometries, conformal transformations constrain the form of the spatial dependence, leading to accurate determinations of the order parameter scaling index, in good agreement with previous independent determinations obtained through standard techniques. The energy density exponent is also computed. [S1063-651X(98)50812-4]

PACS number(s): 64.60.Cn, 05.50.+q, 05.70.Jk, 64.60.Fr

It is well known that quenched randomness can deeply affect the critical properties at second-order phase transitions [1], and is liable to smooth first-order transitions, eventually leading to continuous transitions [2,3].

In random systems, owing to strong inhomogeneities inherent in disorder, the usual symmetry properties required by conformal invariance (CI) [4] do not hold. However, by averaging over disorder realizations (denoted by $[\cdots]_{av}$), translation and rotation invariance are restored, and it is generally believed that conformal invariance techniques should apply in principle. Recent results based on this assumption have recently been obtained at randomness-induced second-order transitions [5,6], but clear evidence of the validity of conformal invariance is still missing. The question is of both fundamental and practical interest. From the fundamental point of view, situations are known where a diverging correlation length *does not guarantee* the validity of CI. A few years ago, lattice animals were indeed found to be *not conformally invariant* although they display isotropic critical behavior with correlation lengths satisfying the usual scaling $\xi \sim L$ with the system size [7]. If conformal invariance works, on the other hand, its powerful techniques might be applied with no restriction to investigate the critical behavior of 2D random systems [8].

In the 2D random-bond Ising model, both analytic [9] and numerical results [10] are available. Transfer matrix (TM) calculations were also used to study the correlation function decay along strips and to compute the conformal anomaly (defined as a universal amplitude in finite-size corrections to the free energy) [11] and, since disorder is marginally irrelevant in the $2d$ Ising model, conformal invariance techniques were indeed efficient. At randomness-induced second-order phase transitions, a direct comparison between the results deduced from conformal invariance, and standard techniques, such as finite-size scaling (FSS) Monte Carlo (MC) simulations, have nevertheless not yet been made. After the pioneering work of Imry and Wortis, the first large-scale MC simulations devoted to the influence of quenched randomness, in a system whose pure version undergoes a strong first-order phase transition, were applied to the case of the eight-state random-bond Potts model (RBPM) [12].

The Hamiltonian of the system with quenched random nearest-neighbor interactions is written: $-\beta\mathcal{H} = \Sigma_{(\mathbf{r},\mathbf{r}')} K_{\mathbf{r}\mathbf{r}'} \delta_{\sigma_{\mathbf{r}},\sigma_{\mathbf{r}'}}$, where the spins, located at sites $\mathbf{r}$ of a square lattice, take the values $\sigma_{\mathbf{r}} = 1,2,\ldots,q$. The coupling strengths are allowed to take two different values K and K'

*Author to whom correspondence should be addressed. Electronic address: berche@lps.u-nancy.fr

$=Kr$ with probabilities p and $1-p$, respectively. If both couplings are distributed with the same probability, $p=0.5$, the system is, on average, self-dual and the critical point is exactly given by duality relations: $(e^{K_c}-1)(e^{K_c r}-1)=q$ [13]. This model has again been carefully investigated recently using both MC simulations [14,15] and TM calculations [16]. The bulk magnetization scaling index $x_\sigma^b=\beta/\nu$ is q dependent [16]. Up to now the most refined direct estimate of x_σ^b in the case $q=8$ is probably a FSS analysis due to Picco ($x_\sigma^b=0.150-0.155$) [15], where it was shown that the random fixed point is reached in the range $r=8-20$, while crossover effects perturb the results outside this domain. As mentioned above, TM calculations have already been performed on the RBPM [16], but with a rather weak disorder $r=2$, leading to $x_\sigma^b=0.142(1)$, while standard FSS results are in the range $x_\sigma^b=0.158-0.175$ [15]. The discrepancy may presumably be attributed to crossover effects.

Due to the increasing literature devoted to second-order induced phase transitions, in this Rapid Communication, our investigation deals with the self-dual eight-state RBPM. We report results of TM calculations on the strip and MC simulations in a square geometry, which support the assumption of conformal covariance of order parameter correlation functions and profiles. We particularly compare independent determinations of the bulk magnetization exponent, resulting in good agreement between standard and conformal invariance techniques. Different large-scale simulations are performed in two types of restricted geometries (strips and squares) with a ratio r chosen in the range $r=8-20$. The crossover regime $r=2$ is also investigated.

In the strip geometry, we used the connectivity transfer matrix formalism of Blöte and Nightingale [17]. For a strip of size L with periodic boundary conditions, the leading Lyapunov exponent follows from the Furstenberg method: $\Lambda_0(L)=\lim_{m\to\infty}(1/m)\ln\|(\Pi_{k=1}^m \mathbf{T}_k)|v_0\rangle\|$, where $\mathbf{T}_k$ is the transfer operator between columns $k-1$ and k, and $|v_0\rangle$ is a suitable unit initial vector. The leading Lyapunov exponent determines the free energy: $f_0(L)=-L^{-1}\Lambda_0(L)$. For a specific disorder realization, the spin-spin correlation function $\langle G_\sigma(u)\rangle=(q\langle\delta_{\sigma_j\sigma_{j+u}}\rangle-1)/(q-1)$, where $\langle\cdots\rangle$ denotes the thermal average, is given by the probability that the spins along some row, at columns j and $j+u$, are in the same state:

$$\langle\delta_{\sigma_j\sigma_{j+u}}\rangle=\frac{\langle 0|\mathbf{g}_j(\Pi_{k=j}^{j+u-1}\mathbf{T}_k')\mathbf{d}_{j+u}|0\rangle}{\langle 0|\Pi_{k=j}^{j+u-1}\mathbf{T}_k|0\rangle},\qquad(1)$$

where $|0\rangle$ is the ground state eigenvector, $\mathbf{T}_k'$ is the transfer matrix in the extended Hilbert space [18], $\mathbf{g}_j$ is an operator that identifies the cluster containing σ_j, and $\mathbf{d}_{j+u}$ gives the appropriate weight depending on whether or not σ_{j+u} is in the same state as σ_j.

It is well known that in disordered spin systems, the strong fluctuations from sample to sample can induce average difficulties [19]. For that reason we paid attention to check, by a careful analysis of the correlation function probability distribution, that self-averaging problems do not alter the mean values [20]. In order to reduce sample fluctuations, we furthermore considered *canonical disorder*, a situation in which exactly the same amount of both couplings is distributed over the bonds of the system. The computations are then performed with 10^6 iterations of the transfer matrix, and the final Lyapunov exponent is averaged over 20 disorder configurations.

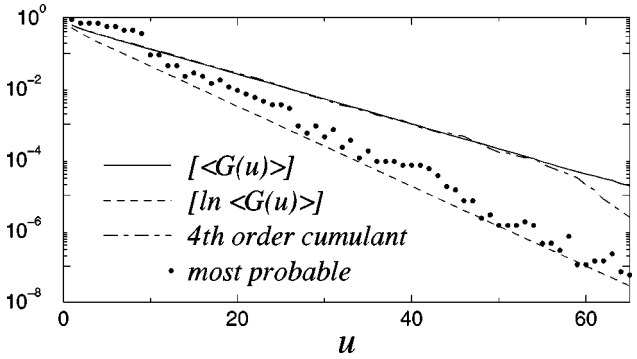

FIG. 1. Average correlation function, most probable value, and fourth-order cumulant expansion, obtained from 63 436 replicas for a strip of size $L=6$ ($r=10$).

Since our purpose is to check the predictions of conformal symmetry, which are supposed to be satisfied by *average quantities*, i.e., $[\langle G_\sigma(u)\rangle]_{av}$, our first aim is to show that, in spite of the lack of self-averaging, our numerical experiments lead to well-defined averages. In Ref. [16], Jacobsen and Cardy argued that in the RBPM, $\ln G$ is self-averaging while G is not. Exploiting duality, they computed $[\ln\langle G_\sigma(u)\rangle]_{av}$ via the free energy of a system in the presence of a seam of frustrated bonds and a cumulant expansion enabled them to deduce the behavior of $[\langle G_\sigma(u)\rangle]_{av}$. In our approach, we are first interested in the probability distribution of the correlation function.

The most probable value $G_\sigma^{mp}(u)$ and the average correlation function $[\langle G_\sigma(u)\rangle]_{av}$, as well as the averaged logarithm $[\ln\langle G_\sigma(u)\rangle]_{av}$, can then be deduced at any value of u. Compatible behaviors are found for $G_\sigma^{mp}(u)$ and $e^{[\ln\langle G_\sigma(u)\rangle]_{av}}$, which confirm the essentially log-normal character of the probability distribution [20], in agreement with Cardy and Jacobsen. It is thus necessary to perform averages over a larger number of samples for $[\langle G_\sigma(u)\rangle]_{av}$ than for $[\ln\langle G_\sigma(u)\rangle]_{av}$ to get the same relative errors. A cumulant expansion enables us to reconstruct $[\langle G_\sigma(u)\rangle]_{av}$ and to compare to the values obtained by averaging directly over the samples. The results in Fig. 1 strengthen the credibility of the direct average and also clearly show that the cumulant expansion up to fourth order still strongly fluctuates compared to $[\langle G_\sigma(u)\rangle]_{av}$.

We will now concentrate on the results that follow from the assumption of conformal covariance of the averaged correlation functions. In the infinite complex plane $z=x+iy$ at the critical point, the correlation function exhibits the usual algebraic decay $[\langle G_\sigma(r)\rangle]_{av}=\text{const}\times r^{-2x_\sigma^b}$, where $r=|z|$. Under a conformal mapping $w(z)$, the correlation functions of a conformally invariant 2D system transforms according to

$$G_\sigma(w_1,w_2)=|w'(z_1)|^{-x_\sigma^b}|w'(z_2)|^{-x_\sigma^b}G_\sigma(z_1,z_2).\qquad(2)$$

The logarithmic tranformation $w=L/2\pi\ln z$ is known to map the z plane onto an infinite strip $w=u+iv$ of width L with periodic boundary conditions in the transverse direction. Ap-

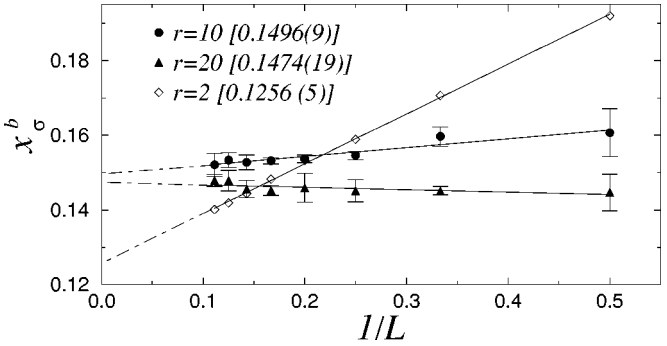

FIG. 2. Magnetic scaling index deduced from the algebraic decay of the average correlation function along the strip of size L as a function of L^{-1}.

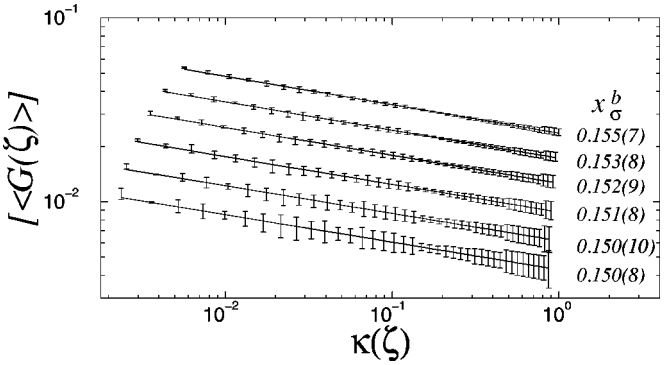

FIG. 3. Rescaled correlation function along six $\omega=$ const curves in the square ($r=10$).

plying Eq. (2) in the random system, one gets the usual exponential decay along the strip $[\langle G_\sigma(u)\rangle]_{av}=\text{const}\times\exp[-(2\pi/L)x_\sigma^b u]$, where the scaling index x_σ^b can be deduced from a semilog plot. For each strip size ($L=2-9$), we realized 40 000 disorder configurations in four independent runs, which allowed us to define mean values and error bars. The exponent follows from an exponential fit in the range $u=5-10L$. For $r=10$, the resulting values plotted against L^{-1}, converge in the $L\to\infty$ limit, towards the final estimate $x_\sigma^b=0.1496\pm0.0009$ shown in Fig. 2. A consistent value is obtained in the case $r=20$, while in the weak disorder limit the behavior is drastically different, and strong crossover effects would be expected for larger strip sizes.

Another restricted geometry, already used in previous FSS MC simulations, is the square geometry. The Schwarz-Christoffel mapping $\zeta=(a/2K)F(z,k)$, $z=\text{sn}[(2K\zeta)/a]\equiv\text{sn}\{[(2K\zeta)/a],k\}$, where $F(z,k)$ is the elliptic integral of the first kind and $\text{sn}(\zeta,k)$ is the Jacobian elliptic sine [21], transforms the upper half plane inside the interior of a square $-a/2\leqslant\text{Re}(\zeta)\leqslant a/2, 0\leqslant\text{Im}(\zeta)\leqslant a$. Here, $K\equiv K(k)$ is the complete elliptical integral of the first kind and the modulus k is a solution of $K(k)/K(\sqrt{1-k^2})=\frac{1}{2}$. The correlation function in the semi-infinite geometry is known to take the form [22]

$$G_\sigma(z_1,z)=\text{const}\times(y_1 y)^{-x_\sigma^b}\psi(\omega), \tag{3}$$

where the dependence on $\omega=y_1 y/|z_1-z|^2$ of the universal scaling function ψ is constrained by the special conformal transformation. In the random situation one can again use the transformation equation (2) to write the correlations between $\zeta_1=i$, close to a side of the square, and any point inside it, as follows:

$$[\langle G_\sigma(\zeta)\rangle]_{av}=\text{const}\times[|\zeta'(z)|\text{Im}(z(\zeta))]^{-x_\sigma^b}\psi(\omega). \tag{4}$$

Taking the logarithm of both sides, the bulk critical exponent x_σ^b can thus be deduced from a linear fit along $\omega=$ const curves in the square:

$$\ln[\langle G_\sigma(\zeta)\rangle]_{av}=\text{const}'-x_\sigma^b\ln\kappa(\zeta)+\ln\psi(\omega), \tag{5}$$

with $\kappa(\zeta)\equiv\text{Im}(z(\zeta))|[1-z^2(\zeta)][1-k^2z^2(\zeta)]|^{-1/2}$.

The results are shown in Fig. 3 ($r=10$), in which the Swendsen-Wang algorithm has been used [23] for systems of size 101×101 and an average was performed over 3000 disorder realizations. Averaging the results at different ω's, one obtains $x_\sigma^b=0.152\pm0.003$. Again, a compatible value is found at $r=20$ while it disagrees at $r=2$.

Owing to the unknown scaling function $\psi(\omega)$, the determination is not extremely accurate, since a few points are used for the fits. It can nevertheless be improved if one considers the magnetization profile inside a square with fixed boundary conditions. Since it is a one-point function, its decay from the distance to the surface in the semi-infinite geometry is fixed, up to a constant prefactor $[\langle\sigma(z)\rangle]_{av}\sim y^{-x_\sigma^b}$. The local order parameter is defined, according to Ref. [24], as the probability for the spin at site ζ in the square, to belong to the majority orientation. After the Schwarz-Christoffel mapping, one gets the following expression for the average profile in the square geometry:

$$[\langle\sigma(\zeta)\rangle]_{av}=\text{const}\times\left(\frac{\sqrt{|1-z^2(\zeta)||1-k^2z^2(\zeta)|}}{\text{Im}(z(\zeta))}\right)^{x_\sigma^b}. \tag{6}$$

This expression, of the form $[\langle\sigma(\zeta)\rangle]_{av}=[f(z)/y]^{x_\sigma^b}$, holds for any point inside the square. It allows an accurate determination of the critical exponent ($x_\sigma^b=0.1499\pm0.0001$ for $r=10$) via a log-log plot shown in Fig. 4. We note that in the case $r=2$, the corresponding curve exhibits a crossover between small and large distances, with clearly different exponents close to 0.128 and 0.160, respectively.

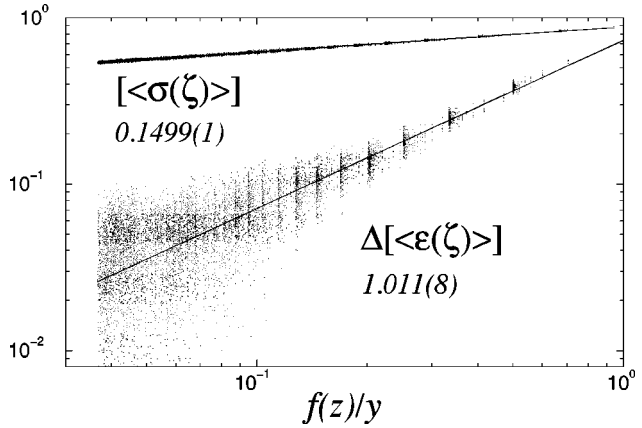

FIG. 4. Rescaled magnetization and energy density profiles inside the square for 3000 disorder realizations ($r=10$). The power law fits are over 100^2 data points.

TABLE I. Comparison between FSS and CI determinations of the bulk magnetic scaling dimension in the $q=8$ RBPM. The quantity that was studied is indicated in the table as well as the geometry and the numerical technique.

FSS (MC)		Conformal invariance			
Square		Strip	Strip	Square	
SW[a] $[\langle M_b\rangle]$	W[b] $[\langle M_b\rangle]$	TM[c] $[\langle G(u)\rangle]$	TM[d] $[\langle G(u)\rangle]$	SW $[\langle G(\zeta)\rangle]$[e]	SW $[\langle \sigma(\zeta)\rangle]$[e]
$r=10$	0.153(1)				
0.153(3)	0.152(2)		0.1496(9)	0.152(3)	0.1499(1)
$r=20$	0.150(1)				
	0.152(2)		0.1474(19)	0.146(7)	0.1462(2)
$r=2$	0.167(2)	0.142(1)			
	0.158(3)	0.142(4)	0.1256(5)	0.283(21)	0.128–0.160

[a]MC simulations (Swendsen-Wang algorithm, $a\leqslant 100$, ~ 500 samples) from Ref. [14].
[b]MC simulations (Wolff algorithm, $\sim 10^5$ samples) from Ref. [15]. The two values refer to fits in the ranges $a=20-100$ and 50–200.
[c]TM calculations ($L=1-7$, 10^2 samples) from Refs. [6,16].
[d]TM calculations ($L=2-9$, 4×10^4 samples), this work.
[e]MC simulations ($a=101$, 3×10^3 samples), this work.

A summary of our results, compared to independent FSS determinations of the magnetic scaling index, are given in Table I. Apart from the crossover regime at $r=2$, the agreement is quite good and clearly in favor of the validity of the assumption of conformal covariance of correlation functions and profiles *at the random fixed point*. On the other hand, in the crossover regime, in which the fixed point is not yet reached, the different techniques lead to different results, and none of them has a real meaning, since they would presumably be affected by strong crossover effects at very large sizes. Since the study of the critical profile with fixed boundary conditions inside the square is very accurate, the energy scaling index $x_\varepsilon^b=d-1/\nu$ can also be obtained through the same technique. This dimension has been calculated in previous studies [6,14] but different results were obtained, possibly contradicting the inequality $x_\varepsilon^b\geqslant 1$. Here, the local energy density $[\langle\varepsilon(\zeta)\rangle]_{av}$ is computed by the average over four bonds on each plaquette. It includes a constant bulk contribution $[\langle\varepsilon_0\rangle]_{av}$, which is obtained by the extrapolation to $y\to\infty$ of the profiles with free and fixed boundary conditions (BC) , respectively. At $r=10$, both BC's yield consistent values $[\langle\varepsilon_0\rangle]_{av}=0.6974$ and 0.6978. The quantity $\Delta[\langle\varepsilon(\zeta)\rangle]_{av}=[\langle\varepsilon(\zeta)\rangle]_{av}-0.6976$ is then studied as in Eq. (6), and leads to $x_\varepsilon^b=1.011\pm 0.008$ (Fig. 4). Since the numerical data are very small, there is an important dispersion but the accuracy of the fit remains correct due to the huge number of data points (100^2).

In this Rapid Communication, we have shown that conformal invariance techniques can be successfully applied to random systems, and that they lead to refined investigations of the critical properties. The accuracy, compared to standard techniques, is increased, especially through the magnetization profile inside a square where all of the lattice points enter the fit. The critical exponents are finally quite close to the rational values $x_\sigma^b=3/20$ and $x_\varepsilon^b=1$.

We thank L. Turban for helpful advice, and M. Henkel and J. L. Cardy for stimulating discussions. The computations were performed at the CNUSC in Montpellier under Project No. C981009 and the CCH in Nancy. The Laboratoire de Physique des Matériaux is a Unité Mixte de Recherche CNRS No. 7556.

[1] A.B. Harris, J. Phys. C **7**, 1671 (1974).
[2] Y. Imry and M. Wortis, Phys. Rev. B **19**, 3580 (1979).
[3] M. Aizenman and J. Wehr, Phys. Rev. Lett. **62**, 2503 (1989); K. Hui and A.N. Berker, *ibid.* **62**, 2507 (1989).
[4] A.A. Belavin, A.M. Polyakov, and A.B. Zamolodchikov, Nucl. Phys. B **241**, 333 (1984).
[5] M. Picco, Phys. Rev. Lett. **79**, 2998 (1997).
[6] J.L. Cardy and J.L. Jacobsen, Phys. Rev. Lett. **79**, 4063 (1997).
[7] J.D. Miller and K. De'Bell, J. Phys. I **3**, 1717 (1993).
[8] *Finite-Size Scaling*, edited by J.L. Cardy (North Holland, Amsterdam, 1988).
[9] B.N. Shalaev, Phys. Rep. **237**, 129 (1994).
[10] W. Selke, L.N. Shchur, and A.L. Talapov, in *Annual Reviews of Computational Physics*, edited by D. Stauffer (World Scientific, Singapore, 1993), Vol. I, p. 17.
[11] S.L.A. de Queiroz and R.B. Stinchcombe, Phys. Rev. B **46**, 6635 (1992); **50**, 9976 (1994); S.L.A. de Queiroz, Phys. Rev. E **51**, 1030 (1995); S.L.A. de Queiroz and R.B. Stinchcombe, *ibid.* **54**, 190 (1996); S.L.A. de Queiroz, J. Phys. A **24**, L443 (1997).
[12] S. Chen, A.M. Ferrenberg, and D.P. Landau, Phys. Rev. Lett. **69**, 1213 (1992); Phys. Rev. E **52**, 1377 (1995).
[13] S. Wiseman and E. Domany, Phys. Rev. E **51**, 3074 (1995).
[14] C. Chatelain and B. Berche, Phys. Rev. Lett. **80**, 1670 (1998).
[15] M. Picco, e-print cond-mat/9802092.
[16] J.L. Jacobsen and J.L. Cardy, Nucl. Phys. B **515**, 701 (1998).
[17] H.W.J. Blöte and M.P. Nightingale, Physica A **112**, 405 (1982).
[18] We used a slightly different technique than Cardy and Jacobsen, whose extended Hilbert space has dimension Lc_L, whereas ours has dimension $(L+3)c_L/2$ (c_L is the dimension of the initial Hilbert space).
[19] B. Derrida, Phys. Rep. **103**, 29 (1984).
[20] A. Crisanti, S. Nicolis, G. Paladin, and A. Vulpiani, J. Phys. A **23**, 3083 (1990).
[21] M. Lavrentiev and B. Chabat, *Méthodes de la Théorie des Fonctions d'une Variable Complexe* (Mir, Moscow, 1972), Chap. VII.
[22] J.L. Cardy, Nucl. Phys. B: Field Theory Stat. Syst. **240**, 514 (1984).
[23] R.H. Swendsen and J.S. Wang, Phys. Rev. Lett. **58**, 86 (1987).
[24] M.S.S. Challa, D.P. Landau, and K. Binder, Phys. Rev. B **34**, 1841 (1986).